BaSO4 Crystals Grown at an Expanding Liquid−Liquid Interface in a Radial Hele-Shaw Cell Show Spontaneous Large-Scale Assembly into Filaments

ARTICLE *in* CRYSTAL GROWTH & DESIGN · MAY 2003

Impact Factor: 4.89 · DOI: 10.1021/cg0255671

6 AUTHORS, INCLUDING:

Debabrata Rautaray
Tata Chemicals Ltd.
31 PUBLICATIONS **997** CITATIONS
SEE PROFILE

Arun Banpurkar
Savirtibai Phule Pune University
43 PUBLICATIONS **561** CITATIONS
SEE PROFILE

S. B. Ogale
CSIR - National Chemical Laboratory, Pune
477 PUBLICATIONS **13,666** CITATIONS
SEE PROFILE

Murali Sastry
Royal DSM
328 PUBLICATIONS **18,741** CITATIONS
SEE PROFILE

CRYSTAL GROWTH & DESIGN
2003
VOL. 3, NO. 4
449−452

$BaSO_4$ Crystals Grown at an Expanding Liquid−Liquid Interface in a Radial Hele-Shaw Cell Show Spontaneous Large-Scale Assembly into Filaments

Debabrata Rautaray,[†] Arun Banpurkar,[‡] Sudhakar R. Sainkar,[†] Abhay V. Limaye,[‡] Satish Ogale,[§] and Murali Sastry*,[†]

Materials Chemistry Division, National Chemical Laboratory, Pune - 411 008, India, Centre for Advanced Studies in Materials Science, Department of Physics, University of Pune, Pune - 411 007, India, and Department of Physics, University of Maryland, College Park, Maryland 20742, USA.

Received August 5, 2002

ABSTRACT: Control over the crystallography, morphology, and spontaneous organization of ceramic crystals are important goals in advanced materials engineering with important application potential. Most studies hitherto have concentrated on static charged interfaces as templates for the controlled nucleation and growth of ceramic crystals. In this communication, we show that $BaSO_4$ crystals grown at a steadily expanding liquid−liquid interface populated by fatty acid molecules spontaneously organize themselves into highly linear superstructures over large length-scales. This experiment is realized in a radial Hele-Shaw cell where the liquid−liquid interfacial growth rate and consequently time scales such as arrival of surfactant molecules to the interface etc. may be readily modulated. Possible reasons for the regular assembly of barite crystals are discussed.

Development of protocols for the synthesis of advanced inorganic materials with control over crystallographic structure, size, and morphology is often driven by commercial requirements in areas as diverse as electronics, pigments and cosmetics, ceramics, and medical industries.[1,2] Insofar as ceramic engineering is concerned, much of the research has centered on the use of templates such as Langmuir monolayers at the air−water[3a−d] and liquid−liquid interface,[3e] self-assembled monolayers,[4] lipid bilayer stacks,[5] and functionalized polymer surfaces[6] to achieve such control. Suitably designed additives in solution during crystal growth have also been used with success in controlling the morphology and structure of ceramic crystals.[5b,7] A relatively unexplored aspect of research in this area concerns the assembly of individual crystallites into highly ordered superstructures, such superstructures often determining the mechanical, optical, and other properties of bioceramic materials such as bone, teeth, and seashells.[7b] Attempts at hierarchical assembly of ceramic crystallites have hitherto mainly relied on synthesis of ceramics such as $BaSO_4$[8] and $BaCrO_4$[9] in microemulsions where interactions between surfactant molecules coating the crystallites were implicated in the assembly process.[8,9]

In templated crystal growth methods,[3−6] the charged interface at which crystal synthesis is carried out is static. To the best of our knowledge, there are no reports investigating the role of an *expanding charged interface* on ceramic crystal growth. We attempt to address this lacuna and demonstrate herein the synthesis of $BaSO_4$ (barite) crystals at the steadily expanding interface between two liquids (aqueous solution of $BaCl_2$ and Na_2SO_4 and chloroform solution containing stearic acid) in a radial Hele-Shaw experiment.[10a] We observe an interesting spontaneous assembly of the barite crystals into very long linear superstructures and speculate on the reasons for such an assembly.

The radial Hele-Shaw cell used in this study comprised two 1-cm-thick, 30 × 30 cm^2 float-glass plates. Spacers of size $b = 300$ μm were used between the top and bottom glass plates. The viscous fluid (mixed aqueous solution of $BaCl_2$ and Na_2SO_4) was placed in the cell gap, and thereafter, chloroform containing stearic acid [$CH_3(CH_2)_{16}COOH$, (1×10^{-2} M)] was injected through a hole (0.5 mm diameter) drilled at the center of the top glass plate using an automated fluid delivery system (Figure 1A). Two experiments were performed in salt solutions as the displaced fluid of supersaturations (S_R) of ca. 30 (5 mL of 1×10^{-3} M aqueous $BaCl_2$ and 5 mL of 3.564×10^{-4} M aqueous Na_2SO_4) and ca. 50 (5 mL of 10^{-3} M aqueous $BaCl_2$ and 5 mL of 9.9×10^{-4} M aqueous Na_2SO_4). A small amount of dye was added to the chloroform to yield sufficient contrast between the aqueous and organic solvent phases for easy capture of the images with the CCD (charge-coupled device) camera (Figure 1A). The experiments were performed at a constant volumetric flow rate (VFR) of chloroform into the aqueous phase (mixed aqueous solutions of $BaCl_2$ and Na_2SO_4) at 0.5 mL/min. The evolution of the finger pattern with time was followed for the above cases using a CCD camera connected to a video recorder at an image capture rate of 25 images/s (Figure 1A). On completion of the injection process (typically 15−20 min), the organic solution was carefully removed and the remaining aqueous precipitate was washed with copious amounts of doubly distilled water and transferred to Si (111) substrates for scanning electron microscopy (SEM)/energy dispersive analysis of X-rays (EDAX)[11] and X-ray diffraction (XRD)[12] measurements. To understand better the role of the surfactant molecules in modulating the morphology and assembly of $BaSO_4$ crystals grown in the Hele-Shaw cell, control experiments were performed wherein the crystallization of $BaSO_4$ was accomplished in the presence of another surfactant (aerosol OT, $C_{20}H_{37}NaO_7S$, 1×10^{-2} M in chloroform) and in the absence of a surfactant in the chloroform phase by maintaining salt solution supersaturation (S_R) at ca. 30 under the same volumetric flow rate used above. In addition to these experiments, another control experiment was performed wherein $BaSO_4$ crystallization was achieved at a *static* liquid−liquid interface in a separating funnel containing a biphasic mixture of 20 mL of a 10^{-2} M stearic acid solution in chloroform and 20 mL aqueous mixture of 10

* To whom all correspondence is to be addressed. Ph: +91 20 5893044. Fax: +91 20 5893952/5893044. E-mail: sastry@ems.ncl.res.in.
[†] National Chemical Laboratory.
[‡] University of Pune.
[§] University of Maryland.

10.1021/cg0255671 CCC: $25.00
Published on Web 05/06/2003

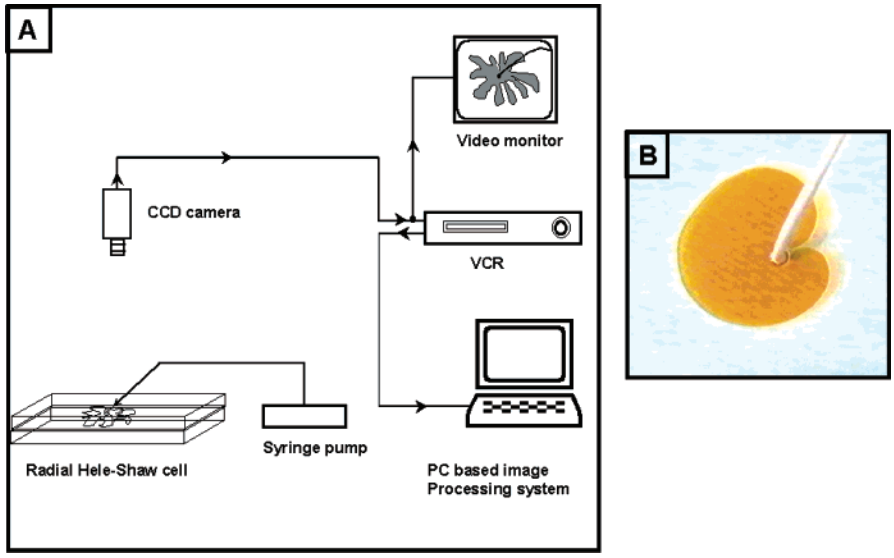

Figure 1. (A) Schematic showing the various elements in the radial Hele-Shaw experiment. (B) Image of the viscous fingering pattern formed at a particular instant during injection of chloroform containing stearic acid (colored phase) into an aqueous solution of $BaCl_2$ and Na_2SO_4 (see text for details).

mL of $BaCl_2$ and 10 mL of Na_2SO_4, the concentrations of the salts were adjusted to yield an S_R of 30. The crystals formed in all the control experiments were transferred onto Si (111) and glass substrates and examined by SEM and XRD.

Figure 1B shows a representative image recorded during injection of chloroform into the electrolyte solution. The interface between the two liquids is very uniform, with no evidence of finger formation. Therefore, on the scale of 10−100 μm, the interface may be considered to be essentially flat. This is an important point to which we will return subsequently. It should be pointed out that the flow rate was decided based upon the induction time observed for initiation of crystal nucleation. The slow VFR coupled with the small difference in viscosities of the two fluids[10b] is responsible for the smooth interface and thus provides a simplified model system for understanding the crystal growth process.

Figure 2A−C show SEM images at different magnifications of $BaSO_4$ crystals grown in the Hele-Shaw cell at an S_R of 30. The representative low magnification SEM image in Figure 2A shows that the substrate is covered with a fairly large density of extremely straight $BaSO_4$ filaments. Figure 2B shows some such $BaSO_4$ filaments (often of lengths in excess of 200−300 μm) criss-crossing the substrate surface. A small percentage of nearly spherical, individual crystallites can also be seen (Figure 2B). At higher magnification, one of the long filaments is observed to consist of assemblies of individual crystallites (Figure 2C). Other smaller filaments at different stages of aggregation are also observed in this image. EDAX analysis of the $BaSO_4$ fibers confirms the expected composition. The XRD pattern recorded from the $BaSO_4$ crystals shown in Figure 2A is displayed in Figure 3, curve 2. A number of Bragg reflections are identified and have been indexed with the reference to the unit cell of the barite structure [$a = 8.8701$ Å, $b = 5.4534$ Å, $c = 7.1507$ Å; space group V_h^{16} ($Pnma$)].[13] For comparison, the simulated powder XRD pattern of barite crystals is shown as curve 1 in Figure 3. An interesting feature of the diffraction pattern of the barite filaments grown in the Hele-Shaw cell is the intense (2 0 0) reflection from the crystals indicating oriented growth of the barite crystals in this experiment (Figure 3, curve 2). During transfer of the barite crystals to the Si (111) substrate, it is reasonable to expect that largest face of the

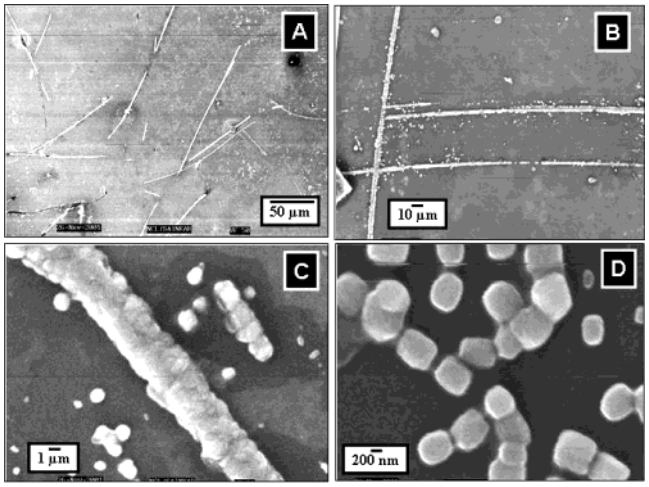

Figure 2. (A−C) Low and high magnification SEM images, respectively, of $BaSO_4$ crystals grown in the Hele-Shaw cell at an S_R of 30 (text for details) and (D) SEM image of $BaSO_4$ crystals grown in the Hele-Shaw cell at an S_R of 50 (text for details).

crystals will lie flat on the substrate surface, and therefore, the orientation of the crystals relative to the liquid−liquid interface in the Hele-Shaw cell is replicated during transfer of the crystals to substrate. The term "oriented growth" is to be interpreted in this sense.

The SEM picture of $BaSO_4$ crystals grown in the Hele-Shaw cell at an S_R of 50 is shown in Figure 2D. While a number of very regular, rectangular $BaSO_4$ crystals densely populating the surface can be seen, the formation of extended linear assemblies of crystallites has not occurred. However, some degree of incipient localized ordering of the rectangular particles can be observed (Figure 2D). EDAX analysis of the $BaSO_4$ rectangular crystals confirms the expected composition. The XRD pattern recorded from the crystals grown at $S_R = 50$ is shown as curve 3 in Figure 3. Barite crystals are formed in this experiment as well. The (2 0 0) reflection is absent, while the (1 1 2) peak is most intense indicating that oriented growth of the crystals in this case is considerably different from that observed in the previous experiment ($S_R = 30$).

A number of physical processes would contribute to crystal growth at the advancing liquid−liquid interface in

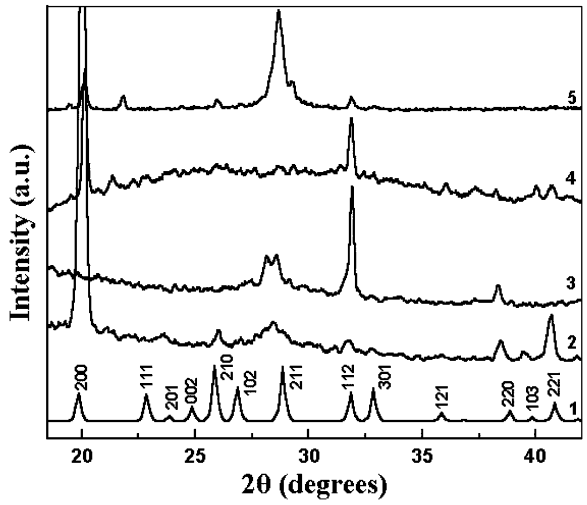

Figure 3. Curve 1: simulated powder XRD pattern of barite crystals; curves 2 and 3: XRD patterns recorded from $BaSO_4$ crystals synthesized in the radial Hele-Shaw cell in the presence of stearic acid at S_R values of 30 and 50, respectively; curve 4: XRD pattern from $BaSO_4$ crystals grown in the Hele-Shaw cell at an S_R of 30 in the presence of AOT; and curve 5: XRD pattern from $BaSO_4$ crystals grown in the Hele-Shaw cell at an S_R 30 in the absence of a surfactant.

the Hele-Shaw experiment. The rate of creation of fresh surface, rate of arrival of stearic acid molecules to the fresh interface, rate of binding of Ba^{2+} counterions to the stearate molecules at the interface, etc.[10b] would influence the nature of barite crystals grown at the interface. By choosing a fixed VFR but different S_R values in a range where supersaturation variation is not expected to lead to significant differences in the morphology of the barite crystals, we expect to understand better growth of the crystals at the expanding interface ($S_R = 30$) versus that occurring in the bulk solution ($S_R = 50$). We believe the linear filaments of barite crystals observed in the $S_R = 30$ Hele-Shaw experiment (Figure 2A−C) correspond to crystals grown at the expanding interface, while the crystals obtained in the $S_R = 50$ experiment are those grown predominantly in the bulk of the electrolyte solution (Figure 2D). To test this hypothesis, control experiments were performed where we did observe barite growth in solution at $S_R = 50$ within 6 min (less than the time-scale of the Hele-Shaw experiment), while no growth in solution was seen at $S_R = 30$ within the same experimental time-scale. The crystal growth process at $S_R = 30$ is similar, in principle, to that reported for barite crystals grown at the air−water interface in the presence of anionic Langmuir monolayers with the difference that the charged interface is now expanding bringing into play the associated time-scale issues mentioned above.[3] We believe the assembly of barite crystals into filamentary superstructures is due to dynamic processes at the interface that are not possible at a static interface such as that provided by Langmuir monolayers. A simple control experiment was performed to test the above hypothesis. $BaSO_4$ crystals were grown at a static liquid−liquid interface as described earlier and the crystals thus obtained were examined by SEM (Supporting Information, S1) and XRD (data not shown). The crystals exhibited a platelike structure, rather similar in morphology to that observed for barite crystals in the Hele-Shaw experiment performed at $S_R = 50$ (Figure 2D), with little evidence for assembly of the individual crystallites into superstructures (S1). As reported in a previous study on the growth of barite crystals at a static liquid−liquid

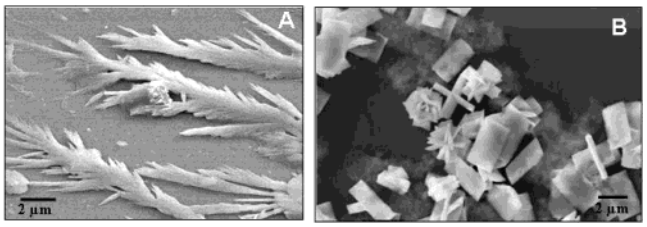

Figure 4. (A) Representative SEM image of $BaSO_4$ crystals grown in the Hele-Shaw cell at an S_R of 30 in the presence of aerosol OT. (B) Representative SEM image of $BaSO_4$ crystals grown in the Hele-Shaw cell at an S_R of 30 in the absence of a surfactant.

interface, in the XRD pattern from the crystals grown at an $S_R = 30$, the (2 0 0) reflection was considerably less intense.[3e]

It is clear from the above that the surfactant at the liquid−liquid interface plays a very important role in directing the crystal morphology. To provide further support for this observation, $BaSO_4$ crystals were grown at the dynamic liquid−liquid interface in the Hele-Shaw cell using the surfactant sodium bis-2-ethylhexyl-sulfosuccinate (aerosol OT, AOT) in the chloroform phase. AOT is a twin-tailed anionic surfactant and is most commonly used to make reverse micelles. A representative SEM picture of $BaSO_4$ crystals grown in the Hele-Shaw cell at an S_R of 30 in the presence of AOT is shown in Figure 4A. The $BaSO_4$ crystals do assemble into extended linear structures with the difference that the assemblies are more branched than in the experiment involving the surfactant stearic acid (Figure 2A−C). Very few individual barite crystallites were observed in the AOT experiment. It is clear from the Hele-Shaw experiments that the expanding liquid−liquid interface plays an important role in assembling the barite crystallites and that the surfactant modulates the morphology of the assembly. The XRD pattern recorded from the $BaSO_4$ crystals shown in Figure 4A is displayed in Figure 3, curve 4. As in the case of barite crystals grown in the Hele-Shaw cell in the presence of stearic acid, an intense (2 0 0) Bragg reflection is observed indicating that oriented growth of the barite crystals is a feature characteristic of nucleation and growth at an expanding liquid−liquid interface.

To differentiate between the ordering influence of an expanding liquid−liquid interface and the presence of surfactant molecules at the interface, a control experiment was performed wherein crystallization of $BaSO_4$ was accomplished in the Hele-Shaw cell at an S_R of 30 in the absence of any surfactant in chloroform phase. The representative SEM image recorded from $BaSO_4$ crystals grown in this experiment is shown in Figure 4B and clearly shows the formation of platelike $BaSO_4$ crystals. It is important to note that there is no evidence for assembly of the crystallites. The XRD pattern recorded from the $BaSO_4$ crystals shown in Figure 4B is displayed in Figure 3, curve 5. These barite crystals exhibited intense (2 1 1) Bragg reflections while the (2 0 0), (2 1 0), and (1 1 2) reflections were comparatively less intense.

There are two important observations based on $BaSO_4$ crystal growth in solution and in the Hele-Shaw cell. The barite crystals that grow at the dynamic liquid−liquid interface in the presence of stearic acid and AOT are not only organized into quasi-linear superstructures (Figures 2A−C and 4A) but they also show preferred orientation along the (200) direction (Figure 3, curves 2 and 4). This preferred orientation is absent in the barite crystals grown in the Hele-Shaw cell in the presence of stearic acid but at a higher S_R of 50 (Figure 3, curve 3) and in the crystals grown in the cell in the absence of a surfactant (Figure 3,

curve 5). The absence of (200) orientation in the crystals grown in the presence of stearic acid at an S_R of 50 can be rationalized in terms of the fact that at this supersaturation value, growth takes place predominantly in the bulk of the solution and not at the interface, as briefly mentioned earlier. A possible mechanism for the assembly of barite crystallites in the Hele-Shaw cell at low S_R values in the presence of stearic acid and AOT could be the following (Figures 2A−C and 4A). It is possible that during movement of the interface, localized hydrodynamic flow effects lead to complete capping of the barite crystals nucleated and grown at the interface. Formation of a monolayer of stearic acid molecules surrounding the barite crystallites could then lead to water-mediated interdigitation of the hydrocarbon chains surrounding the crystallites and association into linear superstructures as observed. That this is indeed a likely mechanism is underlined by the control experiments where such assembly was not observed either in the Hele-Shaw cell experiment performed at a higher S_R (Figure 2D) or in control experiments performed at a static liquid−liquid interface (S1) and in the Hele-Shaw cell in the absence of an ordering surfactant (Figure 4B). As mentioned earlier, the liquid−liquid interface in the Hele-Shaw cell (Figure 1B) is essentially featureless and flat and would explain the linear assembly at the interface mentioned above. A similar mechanism has been put forward for the assembly of $BaCrO_4$ crystallites grown in microemulsions by Mann and co-workers.[9] In the $S_R = 50$ experiment, crystal growth occurs predominantly in the bulk and consequently such an assembly mechanism at the interface is not possible The fact that oriented growth of the barite crystals occurs in the Hele-Shaw cell under conditions where crystal nucleation and growth occurred primarily at the interface indicates epitaxy between the ordering surfactant monolayer at the interface and the (200) face of barite. The observation that preferential growth along the (200) plane occurs both in case of stearic acid and AOT is surprising given that the headgroup packing at the interface would be expected to be different in both cases. Whether hydrodynamic flow effects could play a role in defining growth along preferred crystallographic directions is not clear at this stage. We would like to stress that this communication represents the first step in using a dynamic interface in modulating crystal growth at the interface and the factors mentioned above will be addressed in detail in subsequent reports.

In conclusion, it has been demonstrated that hierarchical assembly of barite crystals nucleated and grown at an expanding interface in the presence of stearate and AOT ions in a radial Hele-Shaw cell results in large-scale assembly of the crystals into filaments of extended dimensions. The barite crystals show growth along a preferred crystallographic direction suggesting epitaxy between the surfactant monolayer at the interface and the crystals. The use of this simple apparatus in materials synthesis at a dynamical one-dimensional chemical boundary can be extended to synthesize submicron wires, which is of considerable current interest. The controlled growth (and indeed assembly) of nanoparticles and biomacromolecules in the Hele-Shaw cell is another exciting possibility and is currently being pursued.

Acknowledgment. D.R. thanks the Department of Science and Technology (DST), Government of India, for financial assistance. This work was partially funded by grants to M.S. from the DST and the Indo-French Centre for the Promotion of Advanced Scientific Research (IFCPAR, New Delhi) and is gratefully acknowledged.

Supporting Information Available: Low and high magnification SEM images of $BaSO_4$ crystals grown at a static liquid−liquid interface containing a biphasic mixture of 20 mL of a 10^{-2} M stearic acid solution in chloroform and 20 mL aqueous mixture of 10 mL of $BaCl_2$ and 10 mL of Na_2SO_4 at an S_R of 30 (S1). This material is available free of charge via the Internet at http://pubs.acs.org.

References

(1) Mann, S.; Ozin, G. A. *Nature* **1996**, *382*, 313.
(2) Matijevic, E. *Curr. Opin. Colloid Interface Sci.* **1996**, *1*, 176.
(3) (a) Heywood, B. R.; Mann, S. *Langmuir* **1992**, *8*, 1492. (b) Heywood, B. R.; Mann, S. *J. Am. Chem. Soc.* **1992**, *114*, 4681. (c) Litvin, A. L.; Valiyaveettil, S.; Kaplan, D. L.; Mann, S. *Adv. Mater.* **1997**, *9*, 124. (d) Buijnsters, P. J. J. A.; Donners, J. J. J. M.; Hill, S. J.; Heywood, B. R.; Nolte, R. J. M.; Zwanenburg, B.; Sommerdijk, N. A. J. M. *Langmuir* **2001**, *17*, 3623. (e) Rautaray, D.; Kumar, A.; Reddy, S.; Sainkar, S. R.; Pawaskar, N. R.; Sastry, M. *CrystEngComm* **2001**, *45*, 1−4.
(4) (a) Kuther, J.; Nelles, G.; Seshadri, R.; Schaub, M.; Butt, H.-J.; Tremel, W. *Chem. Eur. J.* **1998**, *4*, 1834; $CaCO_3$ (b) Aizenberg, J.; Black, A. J.; Whitesides, G. M. *J. Am. Chem. Soc.* **1999**, *121*, 4500.
(5) (a) Sastry, M.; Kumar, A.; Damle, C.; Sainkar, S. R.; Bhagwat, M.; Ramaswamy, V. *CrystEngComm* **2001**, 21. (b) Rautaray, D.; Kumar, A.; Reddy, S.; Sainkar, S. R.; Sastry, M. *Cryst. Growth Des.* **2002**, *2*, 197.
(6) (a) Feng, S.; Bein, T. *Science* **1994**, *265*, 1839. (b) Falini, G.; Gazzano, M.; Ripamonti, A. *Adv. Mater.* **1994**, *6*, 46.
(7) (a) Bromley, L. A.; Cottier, D.; Davey, R. J.; Dobbs, B.; Smith, S.; Heywood, B. R. *Langmuir* **1993**, *9*, 3594. (b) Qi, L.; Coffen, H.; Antonietti, M. *Angew. Chem., Intl. Ed.* **2000**, *39*, 604. (c) Uchida, M.; Sue, A.; Yoshioka, T.; Okuwaki, A. *CrystEngComm* **2001**, 5.
(8) Hopwood, J. D.; Mann, S. *Chem. Mater.* **1997**, *9*, 1819. (b) Li, M.; Mann, S. *Langmuir* **2000**, *16*, 7088.
(9) Li, M.; Schnablegger, H.; Mann, S. *Nature* **1999**, *402*, 393.
(10) (a) The radial Hele-Shaw cell is a simple setup to study the phenomenon of viscous fingering and the factors that control the finger patterns. Such "fingers" are formed during displacement of a viscous fluid by a less viscous one, and this phenomenon has important implications in secondary oil recovery, electrochemical deposition, combustion, and fluid flow in porous media (Ben-Jacob, E.; Garik, P. *Nature* **1990**, *343*, 523 and references therein). While the Hele-Shaw cell has been used extensively in understanding the underlying physics of dynamic instabilities at liquid−liquid interfaces, its use in chemistry in probing surfactant-mediated interfacial recognition events has only recently been attempted (Sastry, M.; Gole, A.; Banpurkar, A. G.; Limaye, A. V.; Ogale, S. B. *Current Sci.* **2001**, *81*, 191). We are not aware of any report on the synthesis of materials in a Hele-Shaw cell. (b) Bonn, D.; Kellay, H.; Amar, B. M.; Meunier, J. *Phys. Rev. Lett.* **1995**, *75*, 2132.
(11) XRD analysis of the $BaSO_4$ samples was carried out on a Philips PW 1830 instrument operating in the transmission mode at 40 kV voltage and a current of 30 mA with CuK_α radiation.
(12) SEM measurements were carried out on a Leica Stereoscan-440 scanning electron microscope equipped with a Phoenix EDAX attachment.
(13) Hill, R. J. *Can. Mineral.* **1977**, *15*, 522.

CG0255671